PHYSICS-BASED SIMULATION WORKFLOW FOR STAMP FORMING OF THERMOPLASTIC PARTS

Rebecca A. Cutting, Justin Hicks, Anthony Favaloro, Eduardo Barocio, Garam Kim, Johnathan E. Goodsell, R. Byron Pipes
Composites Manufacturing and Simulation Center, Purdue University, West Lafayette, IN 47906

Abstract

Stamp forming of thermoplastic composites provides an opportunity for the automotive industry to manufacture light-weight components with superior mechanical properties while achieving a reduced cycle time. Prior to stamping, continuous fiber preforms, called blanks, are consolidated on a press. The forming process entails heating the blanks to a processing temperature, quickly shuttling the blanks to the press, and forming the part with a heated, two-sided mold. The forming pressure is held on the part until it cools to a solid state, and then it is ejected from the tooling and continues to cool to ambient temperature. This paper presents a physics-based simulation workflow for the forming, heat transfer, and subsequent part deformation of a thick, double-curvature part made with CF-PEKK. The forming process and any subsequent wrinkling and fiber reorientation is captured with the software AniForm. The updated fiber angles from the forming simulation are used as inputs for a sequentially coupled thermo-mechanical analysis in Abaqus, which predicts the temperature and crystallinity history of the part during forming and cooling. These results are fed into a mechanical analysis which captures the build-up of residual stresses and subsequent relaxation and deformation of the part as it cools outside of the tool. Finally, the predicted deformation is compared to the experimentally measured warpage of a part made with this manufacturing cycle.

Introduction & Background

Thermoplastic composites offer the promise of high-rate manufacturing to meet the anticipated volume of composite materials in the future. Stamp forming of thermoplastic composites is a high-rate manufacturing process amenable to the automotive industry. Like stamp forming of metals, thermoplastic stamp forming uses pressure and heat to form the composite laminate; hence, the existing stamping infrastructure in the automotive supply chain could be updated to stamp forming composites. In addition to high rate, stamp forming can produce parts with superior mechanical performance, owing to the continuous-fiber architecture of the preform laminate. However, as with metal stamp forming, tooling is expensive and producing a quality part is often an expensive experimental trial-and-error process.

Modeling and simulation offer to reduce the experimental burden and allow science-based design of thermoplastic stamp formed parts, process, and tooling. However, the physics involved in the stamp forming process are numerous, complex, and to-date, no single workflow exists to allow a design engineer to numerically simulate all the phenomenon relevant to the part, manufacturing process, and tool design. Researchers at the Composites Manufacturing and Simulation Center at Purdue University have combined the existing solutions for thermoplastic stamp forming into a prototype workflow with the aim of enabling part, process, and tooling design from a single solution. Physics include: anisotropic thermo-viscoelasticity, polymer crystallization, thermal and crystallization shrinkage, anisotropic heat transfer, part-tool friction, and ply-ply interaction [1–5]. The workflow connects the simulation code AniForm, to simulate the forming process, including tool-part interaction and ply-ply interaction, at forming temperature; and Abaqus, to simulate anisotropic heat transfer, kinetics of polymer crystallization, anisotropic thermo-viscoelasticity, and thermal and crystallization shrinkage of

the composite material [1]–[6]. This workflow enables simulation of the heating and cooling processes, and the subsequent development of crystallinity, shrinkage, residual stresses, and post-forming warpage. The workflow has been exercised to predict the effects of processing, including gripping conditions and thermal history, on part quality, as measured by wrinkle formation and warpage of the formed part.

Materials and Manufacturing Process

The material used for all analyses and manufacturing in this study is AS4-PEKK carbon composite prepreg. Forming of thermoplastic composites is a multi-stage process. The first stage involves cutting each ply to shape and laying them up in a ply-stack. The ply-stack is then heated past melt-point and consolidated under pressure in a heated press, creating what is known as a blank. The blank cools slowly to room temperature and is removed from the consolidation tool. The blank is then transferred to the forming equipment. The blank is held around its edges in a picture frame-like apparatus using a range of possible devices, including mechanical fingers, grips and hooks. These devices assist with holding the blank in the correct location during the heating and forming stages of the manufacturing process. The blank is shuttled into an IR oven where it is heated to a temperature higher than the melt-point of the thermoplastic matrix. When the entire laminate is above the melt temperature, the blank is shuttled at high speed into the press which holds the forming tools. The forming tools and press are heated to control the cooling rate and temperature plateau of the formed part once the tools move into contact with the blank during the final step of the forming process. Double-sided tools form the blank into the part geometry under pressures typically in the range of 500 psi. The part has some excess material remaining around the edges at the conclusion of this step and is, therefore, typically subjected to a machining step to remove the excess and trim the part to its final geometry.

Simulation Framework

The simulation sequence performed in this work begins with the part design. From the designed part geometry and ply table, the outer and inner surfaces are extracted to provide surfaces for tool design, and ply flattening analysis is performed in CATIA to determine the flat ply contours to be used in the forming simulation as well as physically to cut plies to the required shape on a Gerber table. First, a forming simulation is performed in AniForm using the tooling surfaces, flattened ply shapes, and ideal ply fiber angles. The result of the forming simulation is the deformed state of each ply in the part including any reorientation of fiber angles. Next, an ideal 3D mesh of the as-designed part is generated for use in Abaqus. However, the updated fiber angles from the forming simulation are mapped in an in-ply nearest neighbor mapping so that the Abaqus simulation represents the as-manufactured fiber angles. Finally, a sequentially coupled heat transfer then warpage simulation is performed to determine the contribution of thermal and crystallization shrinkage to the as-manufactured part shape.

Forming simulations are performed using the large deformation finite element analysis software AniForm [6–8]. AniForm models the in-plane and bending behavior of each ply in the ply stack as well as the ply-ply interactions and ply-tool interactions. The requisite material information for the simulation was previously characterized by the project sponsor and is proprietary. The flattened ply shapes are 2D geometries, while the tooling surfaces are 3D geometries and lie in the part's design coordinate system. Initial ply and tool alignment are performed using the seed point for ply flattening as a mutual index.

Heat transfer and warpage simulations are performed in Abaqus in a sequentially coupled manner similar to the Purdue CMSC's Additive3D simulation workflow [9–12] First, the local fiber orientation is obtained via mapping from the AniForm simulation. Next, a heat transfer

simulation is performed which accounts for the applied thermal boundary condition history (initial radiant heating, radiant heat losses, convective heat losses, conduction heat losses into the tooling). The material model and properties are implemented in Abaqus user subroutines and are temperature dependent specific heat (UMATHT), temperature dependent orthotropic conductivity (UMATHT), crystallization kinetics (UMATHT in heat transfer, UEXPAN in warpage), thermal and crystallization related expansion strains (UEXPAN), and viscoelasticity (UMAT). In each time increment, the temperature history is used to calculate the crystallization history which in turn affects the viscoelastic behavior and expansion strains. While most of the remaining investigation is related to the deformation of the part, the temperature and crystallinity histories play a major role in determining the deformation. Therefore, representative temperature and crystallinity histories are shown for completeness in Figure 1 for a node located in the center of the part and ply stack as well as a node at the corner of the part in the center of the ply stack. The corner of the part cooled faster than the center of the part, but the crystallinity developed at the same rate for each.

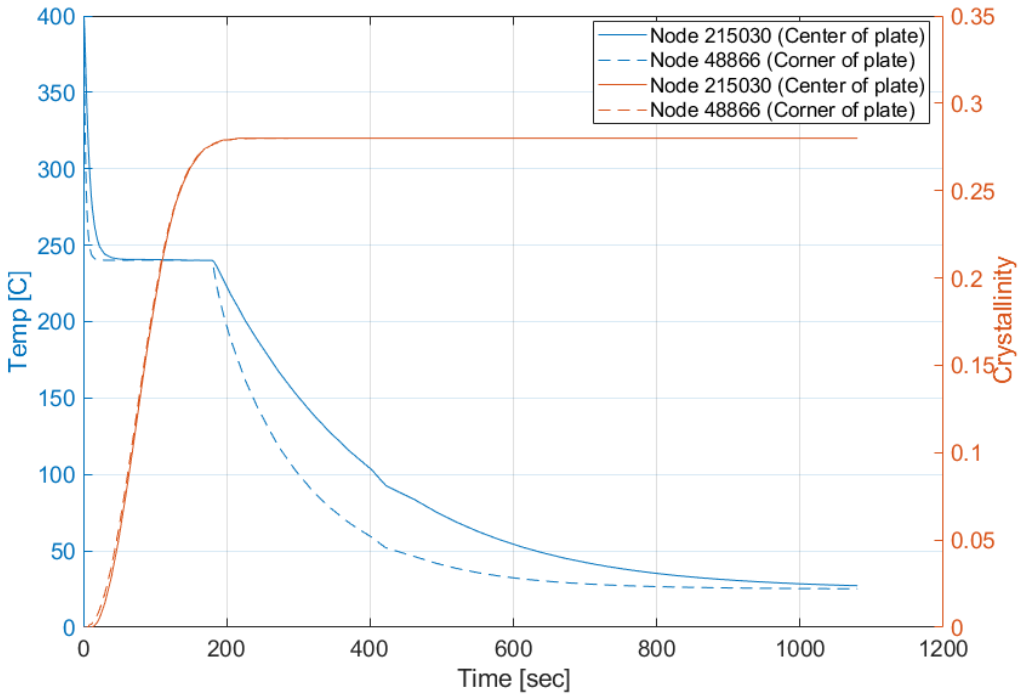

Figure 1: Temperature and crystallinity histories of the center and a corner on the part

Effect of Processing Conditions

The effects of processing conditions including pre-loading of the blank via springs and the temperature of the forming tool on the wrinkles and residual deformation developed in the part after the forming process were investigated using the forming simulation workflow.

Effect of Pre-Loading on Preform

A series of models was developed in AniForm to understand the effect of pre-loading via springs on the forming and subsequent wrinkling of the part. Figure 2 shows the spring configurations tested. The total number of springs varied from 6-12, and up to 3 vertical and 3 horizontal springs were placed per edge. The models contained the same material properties,

analysis mesh, and processing conditions. The only difference between models was the number and location of the springs.

	0V	4V	6V
0H			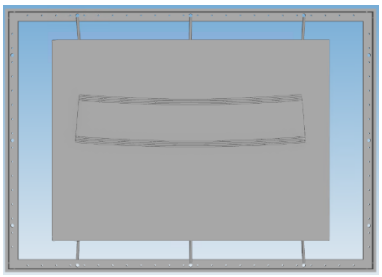
4H		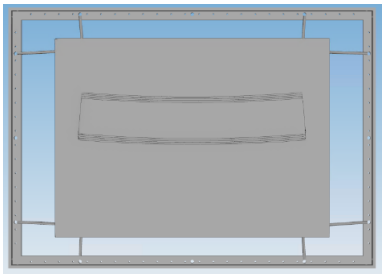	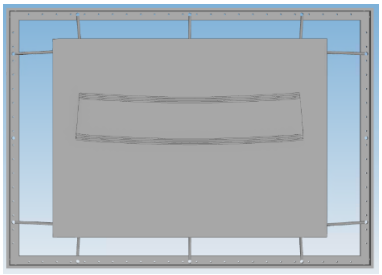
6H	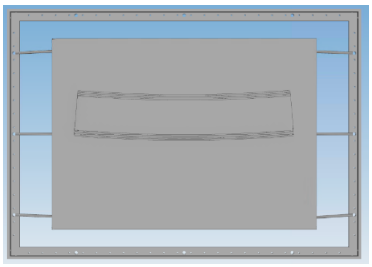	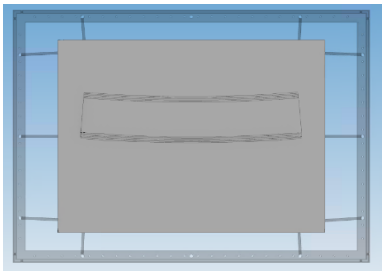	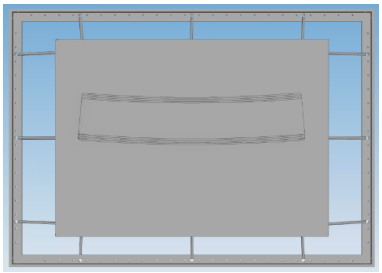

Figure 2: Spring configurations tested in AniForm to look at the effect of pre-loading on wrinkle formation

A change in sign of shear strain can be caused in the part when an out-of-plane wrinkle is flattened into shape conformity. Therefore, identifying locations where shear strain crosses 0 indicates a wrinkle location. Figure 3 shows the shear strain maps for each of the spring configurations, and the legend for the shear strain ranged from -0.1 to 0.1 in order to capture any strain reversals. Every simulation produced wrinkles around the inner ply drop-offs (where the smaller plies are outlined on the interior of the preform). However, the case with 6 horizontal springs and 6 vertical springs (6H-6V) produced the smallest amount of wrinkling in the top center portion of the part of the formed part.

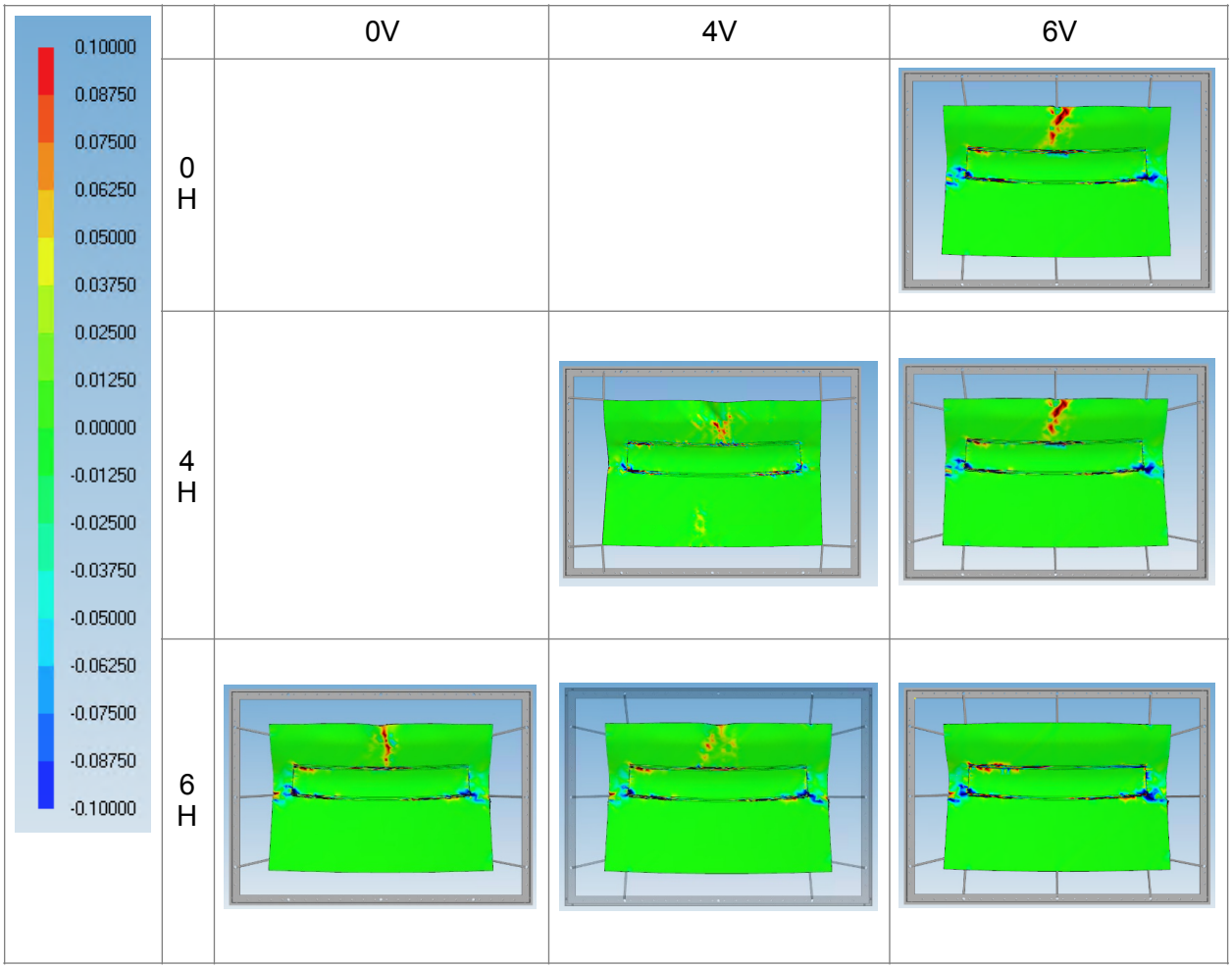

Figure 3: Shear strain reversals on the formed part representing likely locations of wrinkles

The stamped preform has excess material that is trimmed before the part is ready for use. Wrinkling on the excess of the part is less concerning than wrinkling and deformation in the final trimmed part. Figure 4 shows the shape of the stamped AniForm model (black) compared to the as-designed final geometry (blue). The AniForm results mesh was trimmed to match the as-designed final geometry shape, so all deformation comparisons are between parts of the same size.

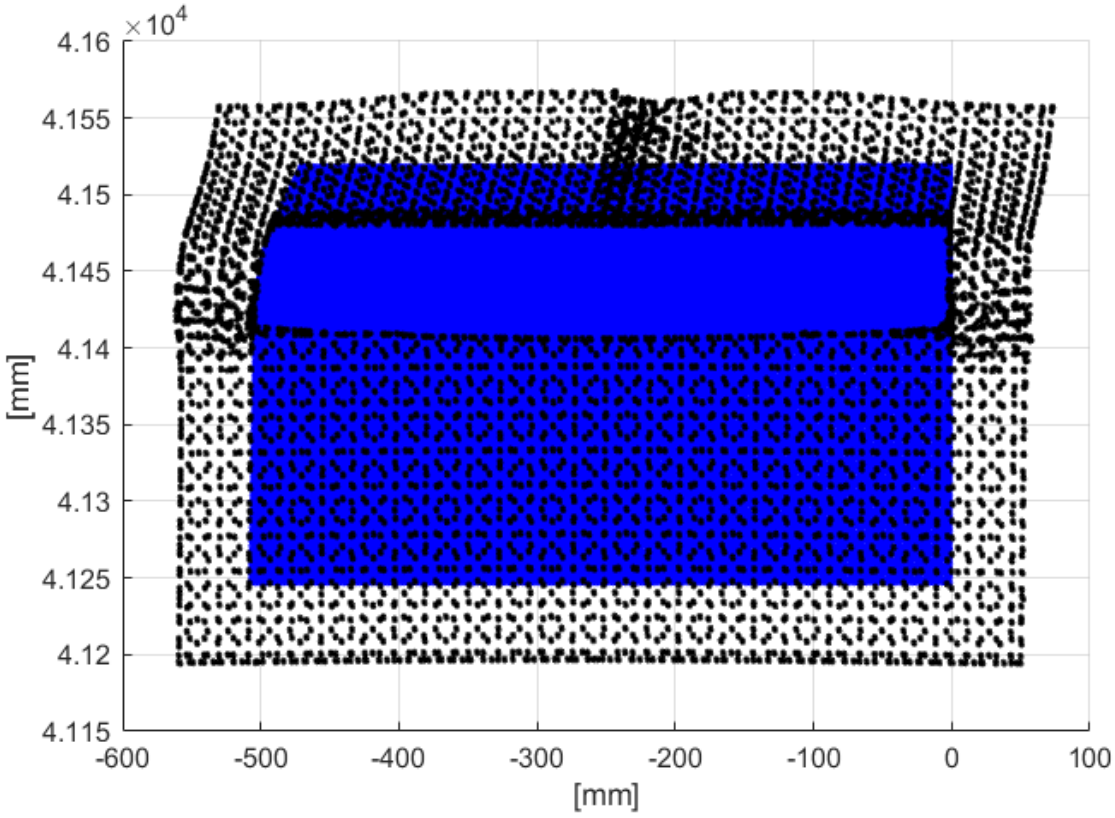

Figure 4: Shape of the stamped preform (black) versus the final trimmed part (blue)

Once the AniForm results mesh was trimmed to represent the final part, the forming simulation results were compared to the as-designed geometry. The nearest neighbor node in the AniForm model was located for every node in the as-designed geometry mesh. The L_1, L_2, and L_∞ norms were calculated for each of the spring configurations, with the norms are defined as:

$$L_1 = \sum \left| distance \right| \quad [1]$$

$$L_2 = \sqrt{\sum distance^2} \quad [2]$$

$$L_\infty = \max(distance) \quad [3]$$

Where the variable $distance$ is an array of the distances between nodes on the AniForm results mesh and the as-designed geometry mesh. These results were normalized and are shown in Table 1- Table 3. The spring configuration with 4 horizontal springs and 6 vertical springs (4H-6V) consistently had the lowest norm. This spring configuration did show more wrinkling in the top portion of the formed shape (see Figure 3) than the 6H-6V spring case.

However, these results compare the final trimmed shape to the as-designed geometry, so some of the wrinkling seen earlier would be removed. These results indicated the best spring configuration was 4H-6V, therefore, this setup was used in the manufacturing process.

Table 1: L_1 norm for total distance between forming simulation results and as-designed geometry

		Vertical Springs		
	L_1	0V	4V	6V
Horizontal Springs	0H			1.040
	4H		1.201	1.000
	6H	1.039	1.039	1.045

Table 2: L_2 norm for total distance between forming simulation results and as-designed geometry

		Vertical Springs		
	L_2	0V	4V	6V
Horizontal Springs	0H			1.036
	4H		1.168	1.000
	6H	1.034	1.035	1.040

Table 3: L_∞ norm for total distance between forming simulation results and as-designed geometry

		Vertical Springs		
	L_∞	0V	4V	6V
Horizontal Springs	0H			1.037
	4H		1.040	1.000
	6H	1.041	1.041	1.026

Effect of Tool Temperature on Warpage

The effect of tool temperature on warpage was also investigated using the sequentially coupled thermo-mechanical analysis performed in Abaqus with the local fiber orientations from the forming simulation mapped over from Aniform. The blank was initialized at the melt temperature of the polymeric matrix ($400\ ^\circ C$) and in the amorphous state (zero crystallinity). Subsequently, a temperature boundary condition was used to represent the temperature of the

forming tool whereas convective and radiative heat transfer mechanisms were applied on the exposed side surfaces of the blank. Similarly, a kinematic boundary condition was applied on one side of the part to represent the geometric constraint imposed by the tool upon forming. Following the forming process, the part was held for five minutes inside the tool and at the tool temperature before it was released. Upon release, convective and radiative heat losses controlled the cooling history of the part from the tool temperature to the ambient temperature. A few nodes were constrained at the center of the part to prevent rigid body motion as internal stresses and deformation developed while cooling down.

The effect of tool temperature on warpage was investigated for five different temperatures equally spaced in a range from $150\ ^{\circ}C$ to $250\ ^{\circ}C$ wherein the lower temperature bound is around the glass transition temperature of the polymeric matrix. Figure 5 shows the magnitude of displacement (mm) from warpage developed by forming the part at three different tool temperatures, $150,\ 200$ and $250\ ^{\circ}C$, and cooling the part to ambient temperature afterwards. The displacement field in Figure 5 shows that the part springs-in in both directions, yet dominantly in the direction with the smallest radius of curvature.

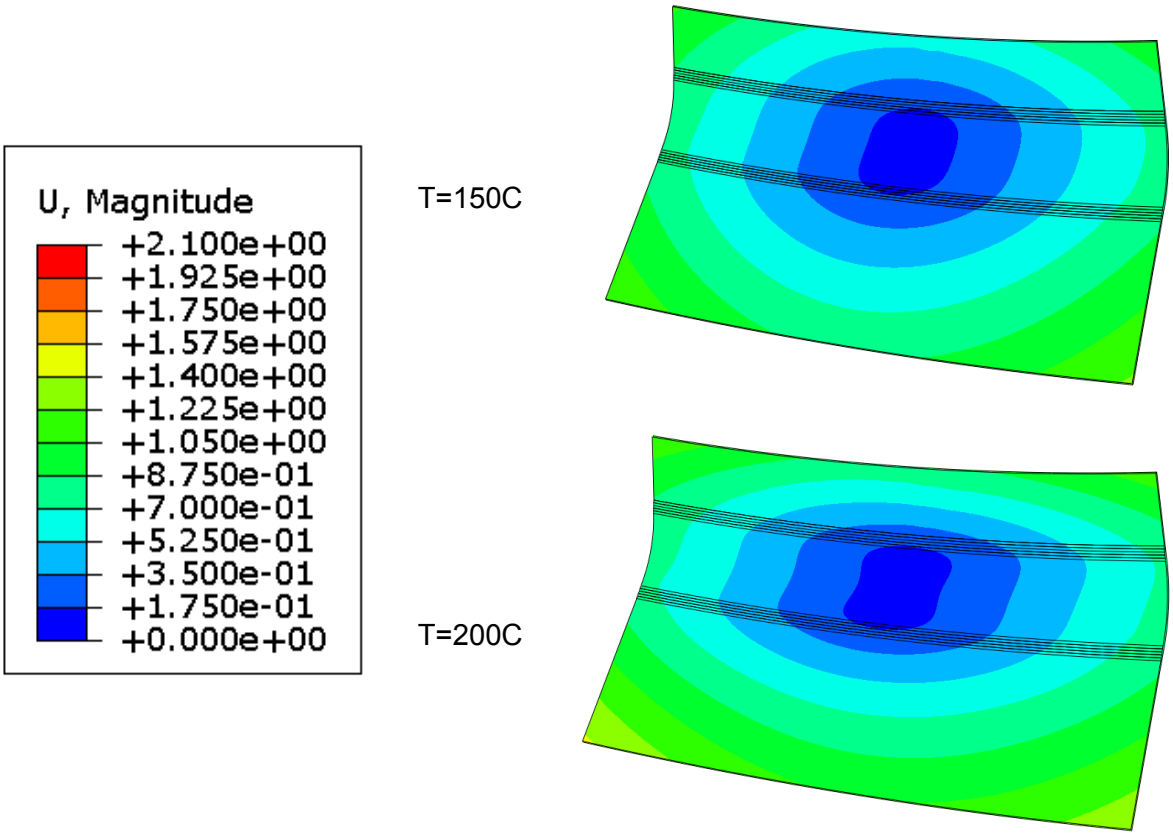

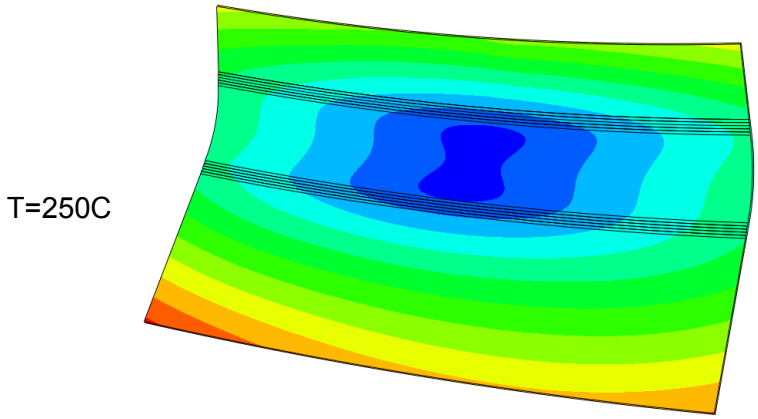

Figure 5: Magnitude of displacement (mm) from warpage developed by forming part at three different tool temperatures and after cooling of the part to the ambient temperature.

Figure 6 shows the maximum displacement (mm) from warpage that resulted from the five tool temperatures investigated. The results clearly show that the larger the temperature difference between the tool and the ambient air, the larger the maximum displacement or spring-in. This behavior agrees with well-established equations for predicting spring-in behavior in laminated composites such as the Radford's equation [13] wherein the angle change is proportional to the temperature difference and the difference in in-plane to through-thickness coefficient of thermal expansion.

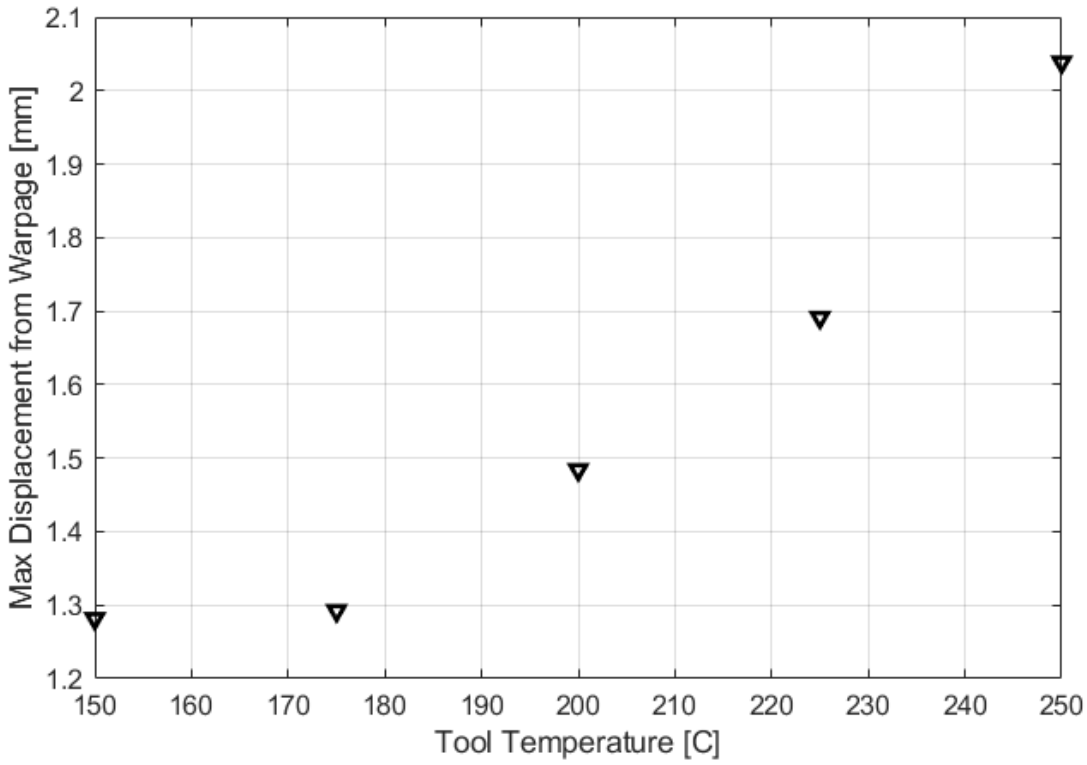

Figure 6: Maximum displacement from warpage developed for different tool temperatures.

Simulation and Manufacturing Outputs

The output of the simulation workflow is used to predict the shape of the as-manufactured part. The sequentially coupled simulated forming process provides a prediction of the final shape of the part by coupling the effects of mechanical forming (simulated in Aniform) and thermal effects during manufacturing (simulated in Abaqus).

An example output (from Aniform) of the simulated displacements in the formed part, including mechanisms such as ply movement, ply-tool interface friction, and ply-ply interactions, is displayed in Figure 7a. These displacements are then added to the deformation outputs from the Abaqus simulation. The simulated output (from Abaqus) of the deformed state of the part are due to the effects of heat transfer on the shrinkage and relaxation of the semi-crystalline polymer and is displayed in Figure 7b. The goal is to compare the combined displacement and warpage results to the as-manufactured shape produced experimentally. An example part that has been manufactured using the thermoplastic composites forming process outlined previously, is displayed in Figure 7c.

(a) Aniform Displacement Results [mm]

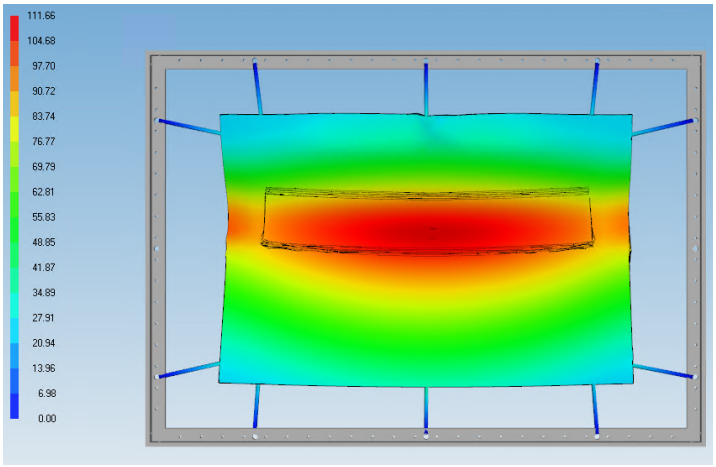

(b) Abaqus Warpage Results [mm]

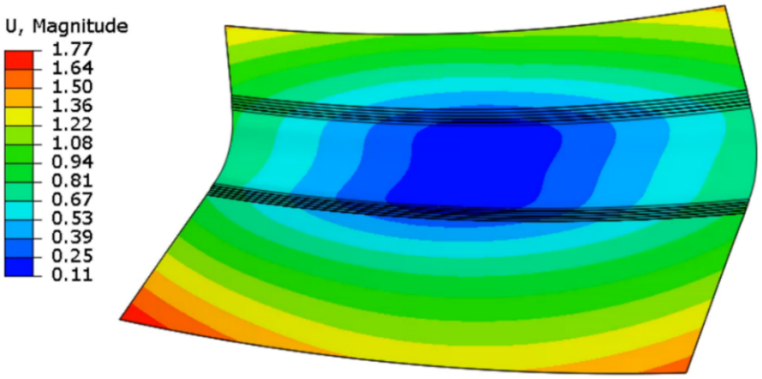

(c) Experimental Results

Figure 7 (a) Simulated Aniform displacement results due to the forming process, (b) Simulated Abaqus warpage results adding the effects of heat-transfer, and (c) An as-manufactured part produced at the Purdue CMSC, created using the thermoplastic composites forming process.

Conclusions

This work presented a simulation workflow for stamp forming of thermoplastic composites using the software AniForm and Abaqus. The forming of a blank at temperature is simulated in AniForm, and the updated geometry (including wrinkles) and fiber orientations are input into a sequentially coupled heat-transfer and warpage analysis. Initial results show that processing conditions like pre-loading on the blank and tool temperature affect the final part shape. The simulation process introduced in this work has the potential to predict manufacturing issues and inform the part, processing cycle, and tooling design. This framework will be used to guide future experimental investigations seeking to improve part quality.

Future work will be completed to validate the simulation workflow. This will involve manufacturing a part under the same conditions as the simulation and characterizing the deformed shape using 3D metrology processes. Additionally, parts will be created with embedded thermocouples in them to collect the time-temperature history at different locations within the laminate. This data will then be used to validate the predicted time-temperature histories and crystallinity development at the same locations in the simulated part throughout the simulation workflow.

Acknowledgements

The authors wish to acknowledge the support of the Boeing Company for our research in the Hybrid Forming of Continuous Fiber Thermoplastic Composites under Purdue University Master Research Agreement No. 2017-036.

Bibliography

1. Velisaris CN, Seferis JC. Crystallization kinetics of polyetheretherketone (peek) matrices. Polymer Engineering & Science 1986;26:1574–81. https://doi.org/10.1002/pen.760262208.
2. Sunderland P, Yu W, MÃ¥nson J-A. A thermoviscoelastic analysis of process-induced internal stresses in thermoplastic matrix composites. Polymer Composites 2001;22:579–92. https://doi.org/10.1002/pc.10561.
3. Chapman TJ, Gillespie JW, Pipes RB, Manson JAE, Seferis JC. Prediction of Process-Induced Residual Stresses in Thermoplastic Composites. Journal of Composite Materials 1990;24:616–43. https://doi.org/10.1177/002199839002400603.
4. Ozisik MN. Heat conduction. John Wiley & Sons; 1993.
5. Greco A, Maffezzoli A. Statistical and kinetic approaches for linear low-density polyethylene melting modeling. Journal of Applied Polymer Science 2003;89:289–95. https://doi.org/10.1002/app.12079.
6. ten Thije R. Finite element simulations of laminated composite forming processes. 2007.
7. ten Thije RHW, Akkerman R. A multi-layer triangular membrane finite element for the forming simulation of laminated composites. Composites Part A: Applied Science and Manufacturing 2009;40:739–53. https://doi.org/10.1016/j.compositesa.2009.03.004.
8. ten Thije RHW, Akkerman R, Huétink J. Large deformation simulation of anisotropic material using an updated Lagrangian finite element method. Computer Methods in Applied Mechanics and Engineering 2007;196:3141–50. https://doi.org/10.1016/j.cma.2007.02.010.
9. Favaloro A, Brenken B, Barocio E, Pipes RB. Simulation of Polymeric Composites Additive Manufacturing using Abaqus. Science in the Age of Experience by Dassault Systemes, 2017.
10. Brenken B, Barocio E, Favaloro A, Kunc V, Pipes RB. Development and validation of extrusion

deposition additive manufacturing process simulations. Additive Manufacturing 2019;25:218–26. https://doi.org/https://doi.org/10.1016/j.addma.2018.10.041.

11. Barocio Vaca E. Fusion Bonding of Fiber Reinforced Semi-Crystalline Polymers in Extrusion Deposition Additive Manufacturing. 2018.
12. Barocio E, Brenken B, Favaloro A, Bogdanor M, Pipes RB. Extrusion Deposition Additive Manufacturing with Fiber-Reinforced Thermoplastic Polymers. In: Friedrich K, Walter R, editors. Structure and Properties of Additive Manufactured Polymer Components. 1st ed., Woodhead Publishing; 2020. 450.
13. Radford DW, Diefendorf RJ. Shape Instabilities in Composites Resulting from Laminate Anisotropy. Journal of Reinforced Plastics and Composites 1993;12:58–75. https://doi.org/10.1177/073168449301200104.